Journal of Hazardous Materials 192 (2011) 915–921

Contents lists available at ScienceDirect

Journal of Hazardous Materials

journal homepage: www.elsevier.com/locate/jhazmat

Promotional effects of carbon nanotubes on V_2O_5/TiO_2 for NO_X removal

Qian Li, Hangsheng Yang*, Famin Qiu, Xiaobin Zhang

State Key Laboratory of Silicon Materials, Department of Materials Science and Engineering, Zhejiang University, Zheda Road 38, Hangzhou 310027, China

ARTICLE INFO

Article history:
Received 27 April 2011
Received in revised form 31 May 2011
Accepted 31 May 2011
Available online 6 June 2011

Keywords:
$DeNO_X$
V_2O_5
SCR
CNTs

ABSTRACT

A series of V_2O_5/TiO_2–carbon nanotube (CNT) catalysts were synthesized by sol–gel method, and their activities for NO_X removal were compared. A catalytic promotional effect was observed by adding CNTs to V_2O_5/TiO_2. The catalyst V_2O_5/TiO_2–CNTs (10 wt.%) showed an NO_X removal efficiency of 89% at 300 °C under a GHSV of 22,500 h^{-1}. Based on X-ray diffraction, scanning electron microscopy, X-ray photoelectron spectroscopy, Raman spectroscopy, NH_3-temperature-programmed desorption, temperature-programmed reduction, Brunauer–Emmett–Teller surface area measurements, differential scanning calorimetry, and thermogravimetric analysis, the increased acidity and reducibility, which could promote NH_3 adsorption and oxidation of NO to NO_2, respectively, contributed to this promotion.

1. Introduction

Nitrogen oxides (NO_X) discharged from power plants, waste incinerators, industrial boilers, engines, and automobiles can result in acid rain, photochemical smog, and ozone depletion. These adverse effects have aroused worldwide attention. Due to the increasing threat of NO_X to the environment, many approaches have been investigated to control NO_X emission. Selective catalytic reduction (SCR) technique has been proven to be one of the most effective methods for reducing NO_X emissions [1,2], although selective non-catalytic reduction (SNCR) has been well applied [3]. A large number of SCR catalysts have been explored, including noble metals [4,5], transition metal oxides [2,6,7], and zeolites [8,9]. Among them, V_2O_5–WO_3/TiO_2 has been extensively used in the industry. The WO_3 is introduced to prohibit catalyst poisoning by sulfur dioxide and also as a catalyst activator [10,11]. However, the operating temperature for these catalysts is usually above 300 °C. Exhaust gases usually contain a large number of fly ash and SO_2, which can easily deactivate the catalysts. Thus, developing active SCR catalysts that can be used at relatively low temperatures (for example below 250 °C) is needed, so that SCR systems could be installed downstream of the desulfurizer and electrostatic precipitator. Low-temperature catalysts contribute to lower energy consumption and help simplify the retrofitting of SCR devices for flue gas cleaning [12].

Recently, many researchers have strived to develop low-temperature catalysts. For example, V_2O_5/activated carbon (AC) [13], V_2O_5/carbon nanotubes (CNTs) [14], Mn–Ce/TiO_2 [15], manganese oxides (MnO_X) [16,17], and MnO_X–CeO_2 [18] have been reported to have high activity at relatively low temperatures. Moreover, CNTs possess unique electronic transportation properties and facile flowing π bond [19,20], which enable them to function as catalytic supports. CNTs have been observed to facilitate elimination of organic pollutants [21,22]. They have also been found to be good NO_X adsorbents [23]. Huang et al. [14] reported that V_2O_5/CNT catalysts showed good activities in the SCR of NO at 373–523 K. In the present study, we report the reduction of NO_X with ammonia over V_2O_5/TiO_2–CNT catalysts, in which TiO_2 and CNTs are used as composite supports. The main purpose of this paper was to elucidate the promotional effect of CNTs on V_2O_5/TiO_2 based catalysts. And the catalysts were pasted on Al plates to form a plate-like structure with parallel channels, which offer certain advantages to large-scale industrial applications: (i) lower pressure drop due to the large open frontal area with parallel channels; (ii) superior attrition resistance and lower tendency to cause plugging of fly ash; and (iii) higher external surface area per unit volume of catalytic reactor [24].

2. Experiments

2.1. Catalyst preparation

The samples were prepared by sol–gel method [11]. Multi-walled carbon nanotubes (MWCNTs) were synthesized by chemical vapor deposition using Co-doped $MgMoO_4$ as catalyst [25,26]. The MWCNTs were purified in concentrated nitric acid for 2 h and then dried and ground for later use. Tetrabutyl titanate and ammonium metavanadate were used as precursors of TiO_2 and V_2O_5, respectively.

* Corresponding author. Tel.: +86 571 87951404; fax: +86 571 87951404.
E-mail address: hsyang@zju.edu.cn (H. Yang).

0304-3894/$ – see front matter © 2011 Elsevier B.V. All rights reserved.
doi:10.1016/j.jhazmat.2011.05.101

Table 1
Summary of the surface element composition and structure property of catalysts.

Material (A, B, C)[a]	Atomic ratio[b] (V, Ti, V/Ti)	CNTs (wt.%)	S (m^2/g)	Pore volume (cm^3/g)	Pore diameter (nm)	Notation
V_2O_5/TiO_2 (0.33, 102, 0)	(0.0053, 0.2048, 1:40)	0	7.4	0.004	3.9	V–Ti
V_2O_5/TiO_2–CNTs (0.33, 97, 1.27)	(0.0018, 0.1679, 1:100)	5	68	0.055	3.2	V–Ti–C-5
V_2O_5/TiO_2–CNTs (0.33, 92, 2.6)	(0.0017, 0.0806, 1:50)	10	74	0.071	3.8	V–Ti–C-10
V_2O_5/TiO_2–CNTs (0.33, 87, 3.8)	(0.0011, 0.0833, 1:75)	15	75	0.086	4.6	V–Ti–C-15
CNTs	–	–	131	0.658	20	CNTs

[a] The letters A and C represent the measured mass of ammonium metavanadate and CNTs, respectively and B represents the measured volume of tetrabutyl titanate.
[b] The atomic ratio was determined by XPS.

Details of catalyst synthesis are as follows. First, purified MWCNTs (1.27–3.8 g), acetic acid (13 mL) and tetrabutyl titanate (97∼87 mL) were ultrasonically dispersed in ethanol for 30 min, ammonium metavanadate (0.3 g) dissolved in oxalic acid and deionized water (4 mL) was added and ultrasonication was continued until a sol was formed. The sol was aged in air for two weeks, and transformed into a gel. The gel was dried at 100 °C and finally calcined at 450 °C for 2 h in N_2 to obtain V_2O_5/TiO_2–CNTs. For comparison, V_2O_5/TiO_2 catalyst was also prepared through the same method. All catalysts were pasted on 10 aluminum plates (3 cm × 10 cm) with 20% organoclay, which were then inserted into a fixed-bed flow reactor. The distance between each plate was approximately 5 mm. The notation and physicochemical properties of catalysts are summarized in Table 1.

2.2. Catalyst characterization

X-ray diffraction (XRD) patterns were recorded on an X-ray diffractometer (Philips XD-98) using Cu Kα radiation (λ = 0.15406 nm). Brunauer–Emmett–Teller surface areas, pore diameter, and pore volume were measured using an ASAP2000 physical adsorber. Sample morphology was characterized by scanning electron microscopy (SEM; JEOL S-4800). X-ray photoelectron spectroscopy (XPS) was conducted on a Kratos Axis Ultra-DLD with Al Kα as radiation source and calibrated by the carbon (1s) line at 284.4 eV. The Raman spectra were obtained on a Labor Raman HR-800 (JDbin Yvon) at 10 mW of the 514.5 nm line of an Ar ion laser to analyze the surface species and the interaction among the metal oxides. Differential scanning calorimetry (DSC) and thermogravimetric analysis (TGA) of V–Ti–C-10 were done on a DSCQ1000 from room temperature to 1000 °C at 10 °C min^{-1} in air.

The temperature-programmed reduction (H_2-TPR) experiment was carried out from 50 to 700 °C in a 1690 Gas Chromatograph using 50 mg of samples. Prior to the analysis, the catalysts were pretreated at 300 °C for 30 min in air. The TPR runs were carried out at a heating rate of 10 °C min^{-1} using a stream of 5% H_2 in argon at a flow rate of 40 mL min^{-1}. The hydrogen consumption was measured by a thermal conductivity detector calibrated with CuO.

The NH_3 temperature-programmed desorption (NH_3-TPD) experiment was performed to determine the acidity of catalysts. A 50 mg of each catalyst was loaded in the reactor and was pretreated in a helium stream (30 mL min^{-1}) at 550 °C for 1 h, and then cooled to 100 °C in the same stream. The pretreated sample was then exposed to NH_3 (4%) at a flow rate of 20 mL min^{-1} for 3 h. The physisorbed NH_3 was removed by flushing the catalysts with N_2 at a flow rate of 30 mL min^{-1} for 1 h before starting the TPD experiment. Experimental runs were recorded by heating the samples in N_2 (30 mL min^{-1}) from 100 to 1000 °C at a heating rate of 10 °C min^{-1}.

2.3. Catalytic activity characterization

An NO–NO_2–NO_X analyzer (Testo AG-testo 350) was used to measure the inlet and outlet concentrations of NO and NO_2. The catalyst temperature was measured using a thermocouple projecting into the center of the reactor. Dry air was used as the source of O_2, and N_2 was used as the balance gas. The premixed gases (1% NO/Ar, 1% NH_3/Ar) were prepared to formulate the flue gas in the experiments. The reaction conditions were as follows: 500 ppm NO, 500 ppm NH_3, 6% O_2, 200 ppm SO_2, and 2.5% H_2O (when used). The reacting gases were mixed and preheated at 100 °C before being introduced into the reactor. The activity measurements were performed from 100 to 300 °C, at increments of 25 °C under the total flow rate of 500 mL min^{-1}, corresponding to the GHSV of 22,500 h^{-1} and the flue gas velocity of approximately 1.0 cm/s. A steady-state experiment was conducted at 300 °C for about 23 h with a GHSV of 22,500 and 33,750 h^{-1}, respectively.

3. Results and discussion

3.1. Catalytic activity

3.1.1. The effect of CNTs on SCR

Fig. 1(a) shows the NO_X conversion as a function of temperature over different catalysts. The V–Ti catalyst presented the lowest activity for reduction of NO_X at 100–300 °C, with the highest removal efficiency of 70% at 300 °C. Its catalytic performance was consistent with other reports [14,27]. The performance of the catalysts increased with the introduction of CNTs. The best performance was achieved with V–Ti–C-10 in the whole temperature range; at temperatures above 175 °C, its NO_X removal efficiencies were at least 20% higher than those of V–Ti under similar conditions.

To evaluate catalytic activity for NO_X conversion, kinetic parameters were calculated according to the simplified Eqs. (1) and (2) based on the assumption that the reaction is first-order dependent on NO_X and zero-order dependent on NH_3, though the reaction is complex, taking into account for the simultaneously occurring of deNO_X and NO_X-formation (through oxidation of NH_3) [3,28,29].

$$k = -\frac{V}{W} \times \ln(1 - x) \quad (1)$$

$$k = A \exp\left(\frac{E_a}{RT}\right) \quad (2)$$

where k is the reaction rate coefficient (mL g^{-1} s^{-1}), V is the total gas flow rate (mL s^{-1}), W is the mass of the catalyst (g), x is the conversion of NO_X (%), E_a is the apparent activation energy (J mol^{-1}), A is the pre-exponential factor, R is the gas constant (8.3145 J mol^{-1} K^{-1}), and T is the temperature (K).

The variation of k with temperature is presented in Fig. 1(b). The values of k for the catalysts V–Ti and V–Ti–C-10 were found to be 2.49 and 3.66, respectively, at 300 °C; this indicates a marked increase in the reaction rate by CNTs. The apparent activation energy for catalysis by V–Ti, V–Ti–C-5, V–Ti–C-10, and V–Ti–C-15 were calculated to be 48.97, 37.78, 32.95, and 34.2 kJ mol^{-1}, respectively, according to the Arrhenius plot. These findings indicate that catalytic reaction was easier over V–Ti–C-10.

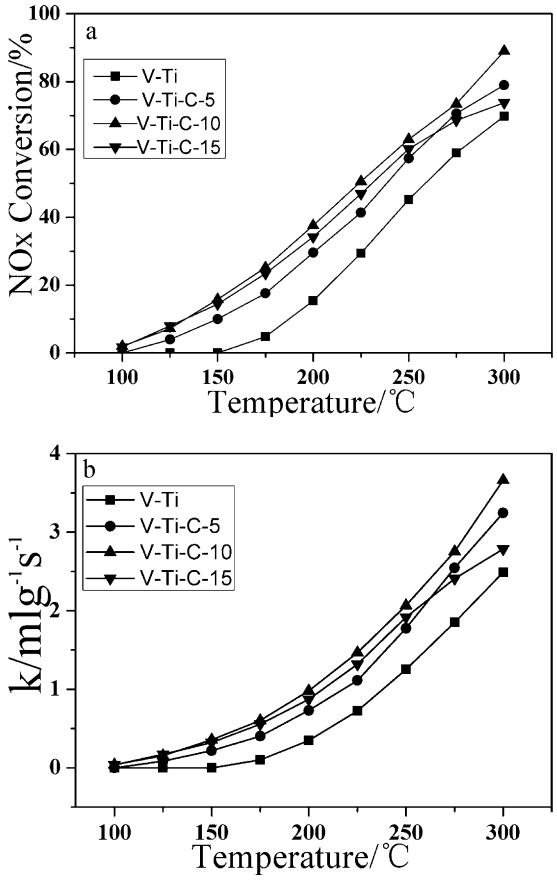

Fig. 1. (a) The NO_X conversion at temperatures over different catalysts. (b) The kinetic rate constant *k* at temperatures over different catalysts. Reaction conditions: NO 500 ppm, NH_3 500 ppm, O_2 6%, N_2 as the balance gas, GHSV = 22,500 h^{-1}.

3.1.2. The effect of CNTs on NO oxidation activity

Oxidation of NO in NO_X removal has gained attention in research. NO_2 is always favored over NO for NO_X removal with NH_3 under oxidizing conditions [2,9]. The SCR rate can be substantially increased when a fraction of NO in the exhaust is converted to NO_2 [28]. A comparison of the efficiency of oxidation of NO to NO_2 with O_2 over different catalysts is shown in Fig. 2. The oxidation of NO to NO_2 over V–Ti increased with temperature. The conversion reached the maximum (35%) at 250 °C, and then decreased with further increase in temperature. The trend of curves for NO oxidation to NO_2 was quite similar among the various catalysts, whereas the conversion of NO to NO_2 increased with the addition of CNTs. The oxidation efficiency of NO to NO_2 over V–Ti–C-10 (61% at 250 °C) was much higher than those over other catalysts. Therefore, the NO_X removal efficiency promotion at temperature below 200 °C could be attributed to the high NO_2 concentration, which promotes the fast reaction of "$2NH_3 + NO + NO_2 = 2N_2 + 3H_2O$". When the temperature is above 200 °C, the reaction of "$8NH_3 + 6NO_2 = 7N_2 + 12H_2O$" also promotes the de$NO_X$ reaction, therefore, high NO_X removal efficiencies are still obtained at high temperatures [30].

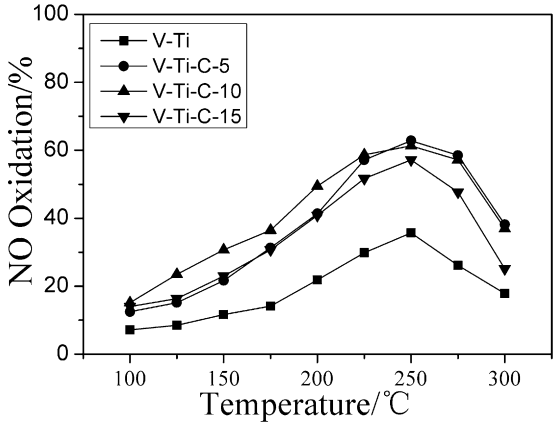

Fig. 2. NO oxidation activity at different temperatures over catalysts. Reaction conditions: 600 ppm NO, O_2 6%, N_2 as the balance, GHSV = 22,500 h^{-1}.

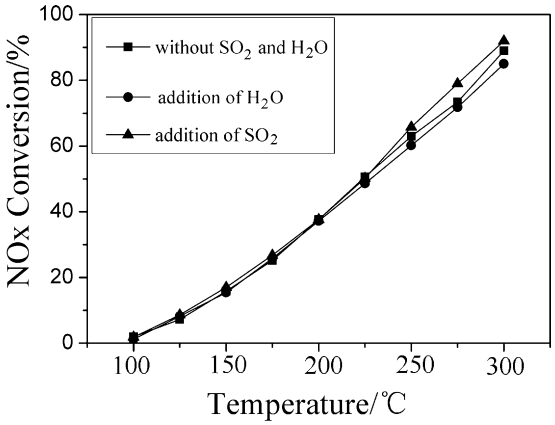

Fig. 3. Catalytic reduction of NO_X at temperatures over catalyst V–Ti–C-10. Reaction conditions: NO 500 ppm, NH_3 500 ppm, O_2 6%, 2.5% H_2O and 200 ppm SO_2 (when used), N_2 as the balance gas, GHSV = 22,500 h^{-1}.

3.1.3. The effect of SO_2 and H_2O on catalysis by V–Ti–C-10

H_2O and SO_2 are common components of industrial exhaust gas; thus, investigating their influence on SCR activity is important. Therefore, transient and steady-state experiments were conducted over V–Ti–C-10. As shown in Fig. 3, when 200 ppm SO_2 was added, NO_X removal increased, especially at high temperatures. This phenomenon was consistent with observations in other reports [13,27,28,31]. This increase could be ascribed to the unstable sulfite formed on the surface of the catalyst, which can react with the chemisorbed oxygen to form sulfate, and thus increase the acidity of catalyst at relatively high temperatures [28,31]. Fig. 3 shows a slight decrease in catalytic activity with the introduction of 2.5% H_2O. This negative effect can be attributed to the adsorption of H_2O on the active sites or to the inhibition of the reaction between NH_3 on Lewis acid sites and NO [27,31].

A positive effect on NO_X removal was observed when 200 ppm SO_2 was introduced to the flue gas under steady state (Fig. 4). When 2.5% H_2O was added, the catalytic property of V–Ti–C-10 slightly decreased. However, no remarkable deactivation occurred when both H_2O and SO_2 were added. When the GHSV was increased from 22,500 (Part I) to 33,750 h^{-1} (Part II), the NO conversion was slightly reduced after several hours of continued testing. According to previous studies [27,30,32], the balance of sulfate salt formation and consumption is the main mechanism that controls the deactivation of the catalyst. The sulfate deposition rate is determined by the balance between its formation and its reaction with NO_X. A high GHSV increased the sulfate formation, which caused an over deposition of sulfate species, thus resulted in the slight reduction of catalytic activity by partly covering the active sites.

3.2. Characterization

3.2.1. Microstructure and morphology analysis

The XRD patterns of V–Ti, V–Ti–C-5, V–Ti–C-10, and V–Ti–C-15 are shown in Fig. 5. The peaks corresponding to TiO_2 (anatase)

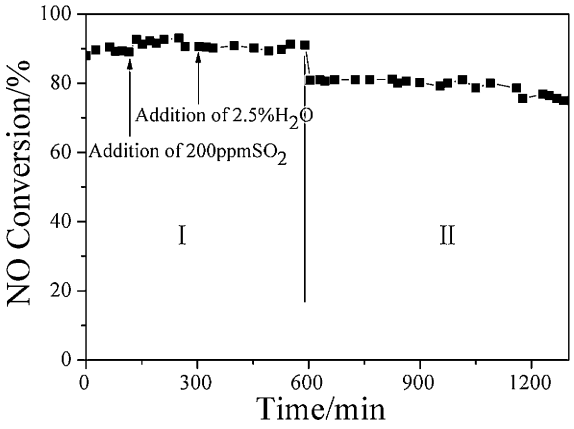

Fig. 4. Catalytic reduction of NO_X at 300 °C over catalyst V–Ti–C-10. Reaction conditions: NO 500 ppm, NH_3 500 ppm, O_2 6%, 200 ppm SO_2, 2.5% H_2O (when used).

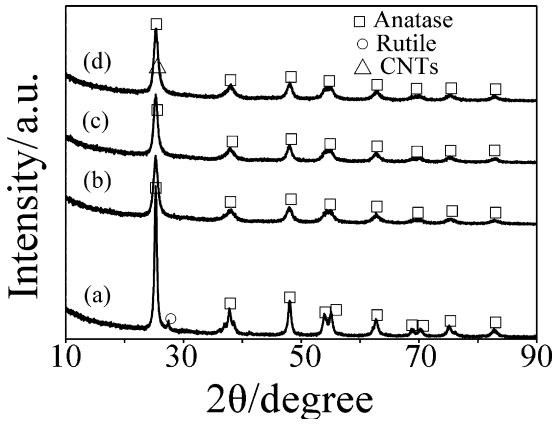

Fig. 5. XRD patterns of the TiO_2-based catalysts. (a) V–Ti; (b) V–Ti–C-5; (c) V–Ti–C-10; (d) V–Ti–C-15.

appeared in the patterns of V–Ti–C-5, V–Ti–C-10, and V–Ti–C-15. The peak at 26.4° is attributed to the peak for CNTs that overlapped with that of TiO_2 at 25.3° [33]. Most peaks for V–Ti were assigned to anatase TiO_2, except for a very small peak corresponding to rutile TiO_2. No peak corresponding to V_2O_5 was observed in all catalysts; this indicates that the amount of its crystalline was too small to be detected. Moreover, the peaks of V–Ti were much sharper than those of the other catalysts. This indicates that the grain size of the catalysts decreased with the addition of CNTs. The crystalline sizes of V–Ti, V–Ti–C-5, V–Ti–C-10, and V–Ti–C-15 calculated from the XRD peaks at 26.4° were 15.3, 9.4, 10, and 9.4 nm, respectively. In summary, the introduction of CNTs reduced the grain size of the catalyst particles, which perhaps contributed to the large specific surface area and good dispersion of catalysts with CNTs.

The specific surface area, pore volume, and pore diameter of the catalysts are summarized in Table 1. Both surface area and pore volume increased with the introduction of CNTs. Although the surface area of the catalysts may not be the determining parameter in SCR activity [17], the high surface area and pore volume may be important to the catalytic reduction of NO_X by NH_3, because high surface area can offer more active sites for reaction.

The V_2O_5 content of the surfaces of V–Ti, V–Ti–C-5, V–Ti–C-10, and V–Ti–C-15 were 7, 0.81, 0.74, and 0.73 μmol m^{-2}, respectively (assuming that all active components were present on the surface of the catalysts). These are lower than values obtained by monolayer coverage (commonly accepted to be 6–7 μmol m^{-2} for vanadia), except for catalyst V–Ti [14].

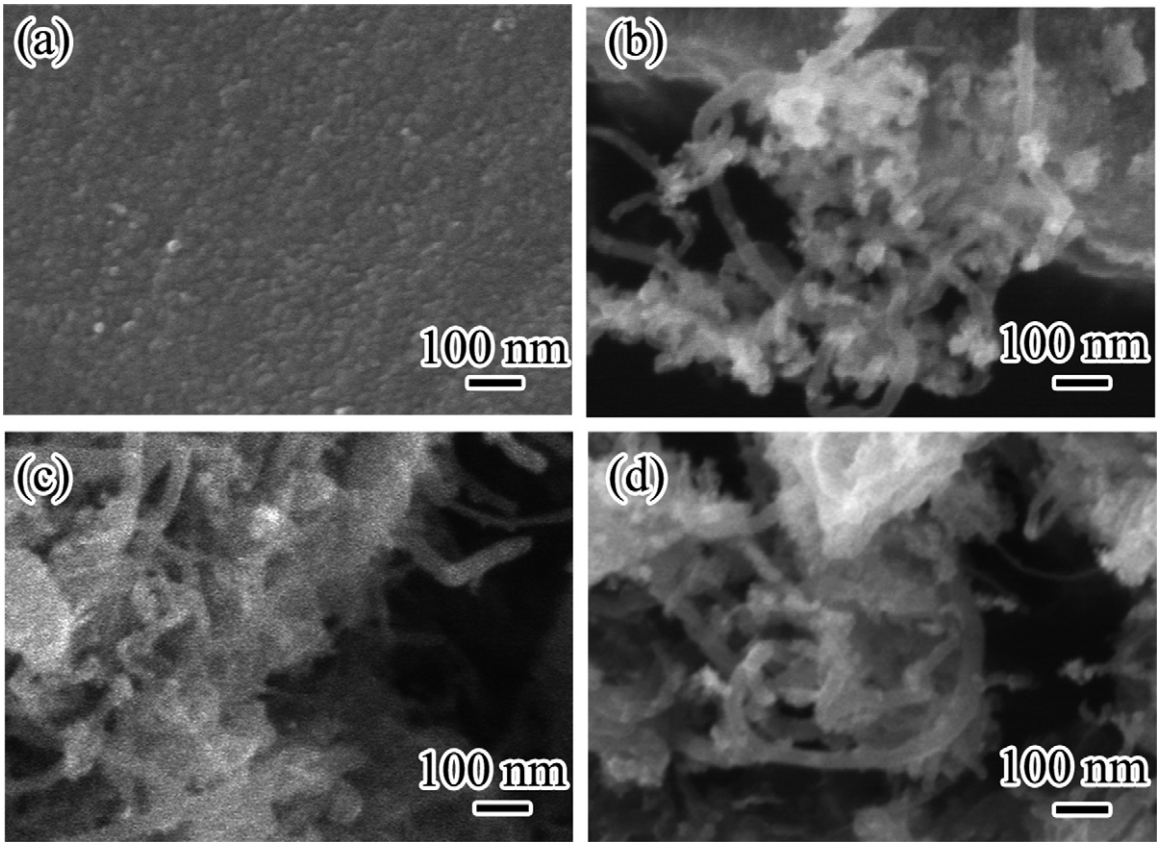

Fig. 6. SEM images of TiO_2-based catalysts. (a) V–Ti; (b) V–Ti–C-5; (c) V–Ti–C-10; (d) V–Ti–C-15.

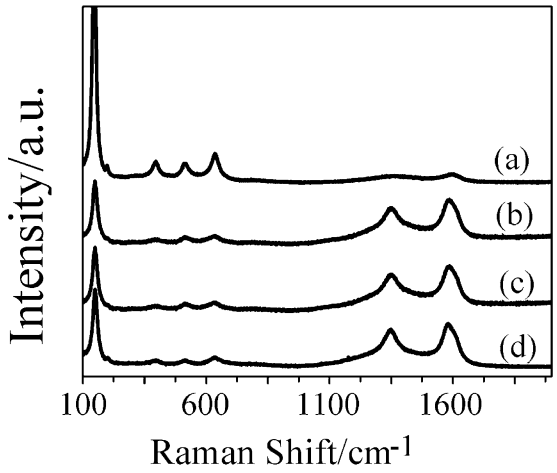

Fig. 7. The Raman spectra of different catalysts. (a) V–Ti; (b) V–Ti–C-5; (c) V–Ti–C-10; (d) V–Ti–C-15.

Fig. 6 shows the SEM images of the catalysts V–Ti, V–Ti–C-5, V–Ti–C-10, and V–Ti–C-15. The mean grain size of V–Ti particles was about 15 nm, and had uniform distribution. When CNTs were introduced, the V_2O_5/TiO_2 particles were dispersedly coated on the surfaces of the CNTs, and their grain size was reduced to ~10 nm.

3.2.2. Surface species analysis

The Raman spectra of the catalysts are shown in Fig. 7. All catalysts produced Raman peaks at 146, 196, 395, 511, and 633 cm^{-1}, which correspond to the anatase phase of TiO_2. Typical Raman peaks of CNTs centered at 1350 (D peak) and 1590 cm^{-1} (G peak) in the spectra of V–Ti–C-5, V–Ti–C-10, and V–Ti–C-15 were detected [34,35]. The intensity of the anatase peaks decreased with the introduction of CNTs; this indicates the reduction of the surface concentration of TiO_2. This implies that the surface coverage of V_2O_5/TiO_2 was reduced by the introduction of CNTs. This was confirmed by the XPS results, as shown in Table 1. Moreover, no Raman peak ascribed to V_2O_5 was observed on all catalyst spectra, which may be due to the low V_2O_5 loading on the surface [34].

The O 1s peaks are displayed in Fig. 8. The peak at 529.6–530.0 eV corresponds to lattice oxygen (hereafter denoted as O_β), whereas the peak at 531.3–531.7 eV corresponds to several O 1s states of surface-adsorbed oxygen (hereafter denoted as O_α) [36]. As shown in Fig. 8, the O_β concentration decreased with the addition of CNTs. The relative concentration ratio of $O_\alpha/(O_\alpha + O_\beta)$ of V–Ti, V–Ti–C-5, and V–Ti–C-10 were calculated to be 0.21, 0.20, and 0.21, respectively. The concentration of chemisorbed oxygen almost remained unchanged with the introduction of CNTs; this form of oxygen,

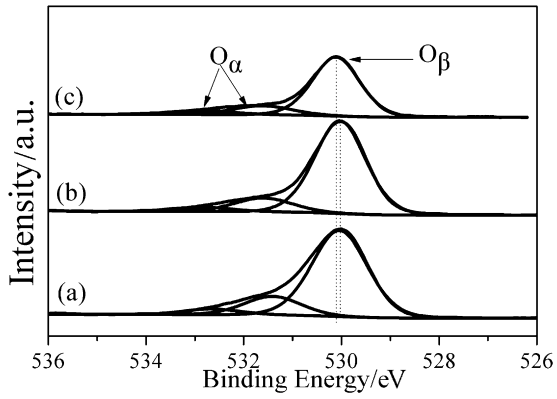

Fig. 8. XPS spectra of O 1s over catalysts. (a) V–Ti; (b) V–Ti–C-5; (c) V–Ti–C-10.

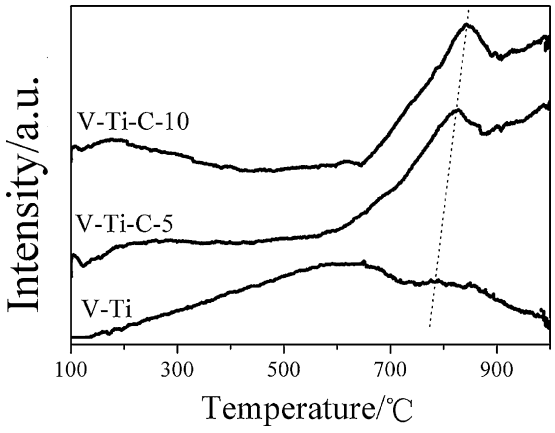

Fig. 9. The NH_3-TPD curves of TiO_2 based catalysts: V–Ti; V–Ti–C-5; V–Ti–C-10.

though, has been suggested to be helpful for SCR [36,37]. The shift of the O_β peak to a higher binding energy suggests a weak interaction between lattice oxygen and metal atoms, which could be beneficial for redox circle and the oxidation of NO to NO_2 in the SCR [37].

3.2.3. Surface acidity

Fig. 9 shows the NH_3-TPD profiles over V–Ti, V–Ti–C-5, and V–Ti–C-10. Two main peaks were observed on V–Ti, namely, a broad peak at ~593 °C and another at ~782 °C. The profiles of V–Ti–C-5 and V–Ti–C-10 were similar, and both produced two peaks centered at 222, 821, 188, and 846 °C. Notably, the peaks centered at ~800 °C shifted to a higher temperature over the catalysts with CNTs. This suggests that the surface acidity of the catalysts was improved. These data clearly indicate that CNTs could increase the acidic strength of the catalyst, and thus facilitate the adsorption and activation of NH_3 during catalysis. Based on the foregoing analysis, we can correlate the acidic strength of the upgraded catalysts to the catalytic activity in the reduction of NO_X [38]. The total amount of acidic sites on V–Ti, V–Ti–C-5, and V–Ti–C-15 were 716, 220, and 185 μmol g^{-1}. The total number of acidic sites of the catalysts did not correlate with the activity of SCR, which was in good agreement with the results of Amiridis et al. [39]. Thus it seems that the strong acid sites contribute to the high catalytic activity in NH_3-deNO_X [40].

3.2.4. Reducibility

Fig. 10 presents the H_2-TPR profiles of V–Ti, V–Ti–C-5, and V–Ti–C-10. A broad peak from 391 to 638 °C was produced by V–Ti, whereas V–Ti–C-5 and V–Ti–C-10 gave rise to sharp peaks at 518

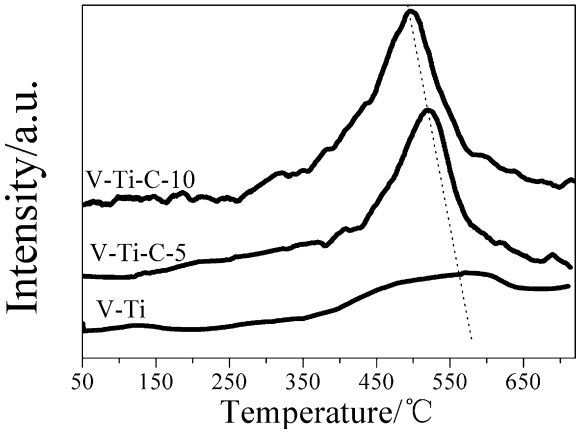

Fig. 10. The H_2-TPR curves of based catalysts: V–Ti; V–Ti–C-5; V–Ti–C-10.

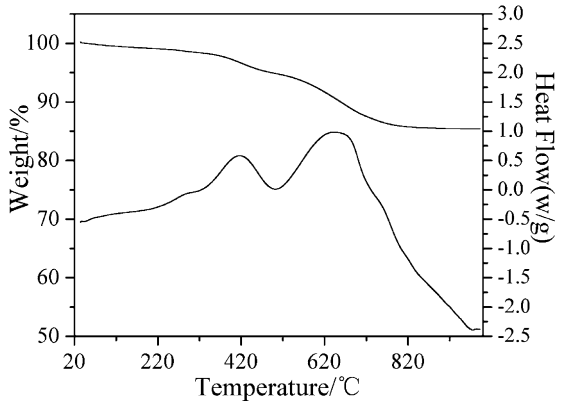

Fig. 11. The TGA–DSC curves of catalyst V–Ti–C-10.

and 497 °C. These peaks can all be ascribed to reduction of vanadia from V^{5+} to V^{3+} [6,37,41]. In contrast to a previous report that several peaks above 627 °C were observed on unsupported V_2O_5 [41], only one peak was observed in our study, which was associated with good dispersion of V_2O_5 on the support. This is in agreement with the XRD results in Fig. 5. The shift of the peaks to lower temperatures indicates that the reducibility of catalysts increased with the addition of CNTs. This is in good agreement with the peak shift of O_β in Fig. 8. This suggests that SCR occurred more easily over V–Ti–C-10 compared with that over V–Ti. The H_2 consumptions of V–Ti, V–Ti–C-5, and V–Ti–C-10 were calculated to be 74, 232, and 497 μmol g^{-1}, respectively. A large increase in H_2 consumption was observed upon addition of CNTs, which probably contributed to the high oxidizing ability of NO and catalytic performance.

3.2.5. Stability

The TGA–DSC curves of V–Ti–C-10 are presented in Fig. 11. The weight loss from room temperature to 200 °C corresponds to the loss of chemisorbed H_2O on the catalyst surface [42]. A small peak at 286 °C on the DSC curve may indicate the oxidation of amorphous carbon in CNTs. A sharp weight loss took place along with the appearance of exothermic peaks at 420 °C, which may be ascribed to the loss of carbonaceous fractures formed during CNTs purification. The peak centered at 650 °C could be assigned to the oxidation of CNTs [23,43]. Based on the TGA–DSC data, the prepared catalyst was stable within 100–300 °C.

4. Conclusions

In summary, SCR activity was significantly promoted by the introduction of CNTs into the traditional catalyst, V_2O_5/TiO_2. The catalyst V_2O_5/TiO_2–CNT (10 wt.%) showed an NO_X removal efficiency of 89% at 300 °C under a GHSV of 22,500 h^{-1}. The addition of CNTs could increase the specific area, pore volume, acidity, and reducibility of the catalysts. Higher reducibility of the upgraded catalyst with CNTs might improve the oxidation of NO to NO_2, and thus contribute to the promotion of NO_X removal. Moreover, V_2O_5/TiO_2–CNTs showed high resistance to SO_2 and H_2O.

Acknowledgments

This work was supported by the Environmentally Sustainable Management of Medical Wastes in China (Contract No. C/V/S/10/251), the National Natural Foundation of Zhejiang Province, China (Grant No. Z4080070), the Foundation of Science and Technology Bureau of Zhejiang Province, China (Grant Nos. 2008C21057 and 2009C34003), and the Fundamental Research Funds for the Central Universities (Program No. 2010QNA4005).

References

[1] V.I. PaÂrvulescu, P. Grange, B. Delmon, Catalytic removal of NO, Catal. Today 46 (1998) 233–234.
[2] H.Q. Wang, J. Wang, Z.B. Wu, Y. Liu, NO catalytic oxidation behaviors over $CoOx/TiO_2$ catalysts synthesized by sol–gel method, Catal. Lett. 134 (2010) 295–296.
[3] S. Mahmoudi, J. Baeyens, J.P.K. Seville, NO_x formation and selective non-catalytic reduction (SNCR) in a fluidized bed combustor of biomass, Biomass Bioenergy 34 (2010) I393–I409.
[4] J.H. Lee, S.J. Schmieg, S.H. Oh, Improved NOx reduction over the staged Ag/Al_2O_3 catalyst system, Appl. Catal. A: Gen. 342 (2008) 78–86.
[5] M. Itoha, M. Saitoa, M. Takeharaa, K. Motoki, J. Iwamotob, K. Machidaa, Influence of supported-metal characteristics on de-NOx catalytic activity over Pt/CeO_2, J. Mol. Catal. A: Chem. 304 (2009) 159–165.
[6] L. Casagrande, L. Lietti, I. Nova, P. Forzatti, A. Baiker, SCR of NO by NH_3 over TiO_2-supported V_2O_5–MoO_3 catalysts: reactivity and redox behavior, Appl. Catal. B: Environ. 22 (1999) 63–77.
[7] Z.B. W.U., B.Q. Jiang, Y. Liu, H.Q. Wang, R.B. Jin, DRIFT study of manganese/titania-based catalysts for low-temperature selective catalytic reduction of NO with NH_3, Environ. Sci. Technol. 41 (2007) 5812–5817.
[8] O. Kröcher, M. Elsener, Combination of V_2O_5/WO_3–TiO_2, Fe-ZSM5, and Cu-ZSM5 catalysts for the selective catalytic reduction of nitric oxide with ammonia, Ind. Eng. Chem. Res. 47 (2008) 8588–8593.
[9] J.H. Li, R.H. Zhu, Y.S. Cheng, C. Lambert, R. Yang, Mechanism of propene poisoning on Fe-ZSM-5 for selective catalytic reduction of NOx with ammonia, Environ. Sci. Technol. 44 (2010) 1799–1805.
[10] K. Everaert, J. Baeyens, Catalytic combustion of volatile organic compounds, J. Hazard. Mater. 109 (2004) 113–139.
[11] K. Everaert, M. Mathieu, J. Baeyens, E. Vansant, Combustion of chlorinated hydrocarbons in catalyst-coated sintered metal fleece reactors, J. Chem. Technol. Biotechnol. 78 (2003) 167–172.
[12] B.W.-L. Jang, J.J. Spivey, M.C. Kung, H.H. Kung, Low-temperature NOx removal for flue gas cleanup, Energy Fuels 11 (1997) 299–306.
[13] Z.P. Zhu, Z.Y. Liu, S.J. Liu, H.X. Niu, Catalytic NO reduction with ammonia at low temperatures on V_2O_5/AC catalysts: effect of metal oxides addition and SO_2, Appl. Catal. B: Environ. 30 (2001) 267–276.
[14] B. Huang, R. Huang, D.J. Jin, D.Q. Ye, Low temperature SCR of NO with NH_3 over carbon nanotubes supported vanadium oxides, Catal. Today 126 (2007) 279–283.
[15] R. Jin, Y. Liu, Z.B. Wu, H.Q. Wang, T.T. Gu, Low-temperature selective catalytic reduction of NO with NH_3 over Mn–Ce oxides supported on TiO_2 and Al_2O_3: a comparative study, Chemosphere 78 (2010) 1160–1166.
[16] X.L. Tang, J.M. Hao, W.G. Xu, J.H. Li, Low temperature selective catalytic reduction of NOx with NH_3 over amorphous MnOx catalysts prepared by three methods, Catal. Commun. 8 (2007) 329–334.
[17] J.H. Li, J.J. Chen, R. Ke, C.K. Luo, J.M. Hao, Effects of precursors on the surface Mn species and the activities for NO reduction over $MnOx/TiO_2$ catalysts, Catal. Commun. 8 (2007) 1896–1900.
[18] G. Qi, R.T. Yang, Characterization and FTIR studies of MnOx–CeO_2 catalyst for low-temperature selective catalytic reduction of NO with NH_3, J. Phys. Chem. B 108 (2004) 15738–15747.
[19] N.M. Rodriguez, M.S. Kim, R.T.K. Baker, Carbon nanofibers: a unique catalyst support medium, J. Phys. Chem. 98 (1994) 13108–13111.
[20] J.M. Planeix, N. Coustel, B. Coq, Application of carbon nanotubes as supports in heterogeneous catalysis, J. Am. Chem. Soc. 116 (1994) 7935–7936.
[21] W. Tian, H.S. Yang, X.Y. Fan, X.B. Zhang, Low-temperature catalytic oxidation of chlorobenzene over MnO_X/TiO_2–CNTs nano-composites prepared by wet synthesis methods, Catal. Commun. 11 (2010) 1185–1188.
[22] X.Y. Fan, H.S. Yang, W. Tian, A.M. Nie, T.F. Hou, F.M. Qiu, X.B. Zhang, Catalytic oxidation of chlorobenzene over $MnOx/Al_2O_3$–carbon nanotubes composites, Catal. Lett. 141 (2011) 158–162.
[23] S. Santucci, S. Picozzi, F.D. Gregorio, L. Lozzi, NO_2 and CO gas adsorption on carbon nanotubes: experiment and theory, J. Chem. Phys. 119 (2003) 10904–10910.
[24] P. Forzatti, Present status and perspectives in de-NOx SCR catalysis, Appl. Catal. A: Gen. 222 (2001) 221–236.
[25] W.J. Guan, Y. Li, Y.Q. Chen, X.B. Zhang, G.Q. Hu, Glucose biosensor based on multi-wall carbon nanotubes and screen printed carbon electrodes, Biosens. Bioelectron. 21 (2005) 508–512.
[26] Y. Li, X.B. Zhang, X.Y. Tao, J.M. Xu, F. Chen, W.Z. Huang, F. Liu, Growth mechanism of multi-walled carbon nanotubes with or without bundles by catalytic deposition of methane on Mo/MgO, Chem. Phys. Lett. 386 (2004) 105–110.
[27] Z.G. Huang, Z.P. Zhu, Z.Y. Liu, Q.Y. Liu, Formation and reaction of ammonium sulfate salts on V_2O_5/AC catalyst during selective catalytic reduction of nitric oxide by ammonia at low temperatures, J. Catal. 214 (2003) 213–219.
[28] J.H. Goo, M.F. Irfan, S.D. Kim, S.C. Hong, Effects of NO_2 and SO_2 on selective catalytic reduction of nitrogen oxides by ammonia, Chemosphere 67 (2007) 718–723.
[29] X.Y. Guo, C. Bartholomew, W. Hecker, L.L. Baxter, Effects of sulfate species on V_2O_5/TiO_2 SCR catalysts in coal and biomass-fired systems, Appl. Catal. B: Environ. 92 (2009) 30–40.
[30] M. Colombo, I. Nova, E. Tronconi, A comparative study of the NH3-SCR reactions over a Cu-zeolite and a Fe-zeolite catalyst, Catal. Today 151 (2010) 223–230.

[31] Z.G. Huang, Z.P. Zhu, Z.Y. Liu, Combined effect of H_2O and SO_2 on V_2O_5/AC catalysts for NO reduction with ammonia at lower temperatures, Appl. Catal. B: Environ. 39 (2002) 361–368.
[32] Z.G. Huang, Z.Y. Liu, X.L. Zhang, Q.Y. Liu, Inhibition effect of H_2O on V_2O_5/AC catalyst for catalytic reduction of NO with NH_3 at low temperature, Appl. Catal. B: Environ. 63 (2006) 260–265.
[33] S. Wang, L.J. Ji, B. Wu, Q.M. Gong, Y.F. Zhu, J. Liang, Influence of surface treatment on preparing nanosized TiO_2 supported on carbon nanotubes, Appl. Surf. Sci. 255 (2008) 3263–3266.
[34] J.A. Martín, M. Yates, P. Ávila, S. Suárez, J. Blanco, Nitrous oxide formation in low temperature selective catalytic reduction of nitrogen oxides with V_2O_5/TiO_2 catalysts, Appl. Catal. B: Environ. 70 (2007) 330–334.
[35] X.Y. Tao, X.B. Zhang, J.P. Cheng, F. Liu, Synthesis and characterization of Cu filled carbon nanohorns, Mater. Chem. Phys. 104 (2007) 210–214.
[36] M. Kang, E.D. Park, J.M. Kim, J.E. Yie, Manganese oxide catalysts for NO_x reduction with NH_3 at low temperatures, Appl. Catal. A: Gen. 327 (2007) 261–269.
[37] L. Chen, J.H. Li, M.F. Ge, Promotional effect of Ce-doped V_2O_5–WO_3/TiO_2 with low vanadium loadings for selective catalytic reduction of NOx by NH_3, J. Phys. Chem. C 113 (2009) 21177–21184.
[38] N.V. Economidis, D.A. Peña, P.G. Smirniotis, Comparison of TiO_2-based oxide catalysts for the selective catalytic reduction of NO: effect of aging the vanadium precursor solution, Appl. Catal. B: Environ. 23 (1999) 123–134.
[39] M.D. Amiridis, R.V. Duevel, I.E. Wachs, The effect of metal oxide additives on the activity of V_2O_5/TiO_2 catalysts for the selective catalytic reduction of nitric oxide by ammonia, Appl. Catal. B: Environ. 20 (1999) 111–122.
[40] W. Tian, H.S. Yang, X.Y. Fan, X.B. Zhang, Catalytic reduction of NOx with NH_3 over different-shaped MnO_2 at low temperature, J. Hazard. Mater. 188 (2011) 105–109.
[41] M.A. Reiche, E. Ortelli, A. Baiker, Vanadia grafted on TiO_2–SiO_2, TiO_2 and SiO_2 aerogels structural properties and catalytic behaviour in selective reduction of NO by NH_3, Appl. Catal. B: Environ. 23 (1999) 187–203.
[42] P. Lin, Q.J. She, B.L. Hong, X.J. Liu, Y.N. Shi, Z. Shi, M.S. Zheng, Q.F. Dong, The nickel oxide/CNT composites with high capacitance for supercapacitor, J. Electrochem. Soc. 157 (2010) 818–823.
[43] A. Misra, P.K. Tyagi, M.K. Singh, D.S. Misra, FTIR studies of nitrogen doped carbon nanotubes, Diamond Relat. Mater. 15 (2006) 385–388.